Simulation of negative pressure behavior using different shapes and positions of pressure inlet and seed hole diameters using ANSYS-CFX to optimize the structure of a pneumatic metering device designed for wheat

Satti Hassan Yasir[1,2]   Qingxi Liao[1*]

(1. Huazhong Agricultural University (HAZU), Wuhan, China;

2. University of Dongola, Northern state, Sudan)

Abstract: The pneumatic precision metering device for wheat was innovated, designed and tested under laboratory conditions. Very good results were then obtained according to the precision seeding criteria based on quality of feed index (QFI), miss index (MIS) and multiple indexes (MULI).   To optimize the structure of the design for gas stability before manufacturing, ANSYS-CFX was involved. Gas behavior was simulated under different shapes and positions for pressure inlet along with different seed hole diameters.

According to the structure determined in ANSYS-CFX, the seed hole of 1.8 mm and cylindrical shape of pressure inlet was found to be the best among others, accordingly the device was then manufactured and tested under laboratory and field conditions.   The results from laboratory and field experiments were found to be in conformity with these of simulation, which indicated that ANSYS-CFX is a powerful and highly accurate application in optimizing the structure of such designs.

Keywords: simulation, precision metering device, negative pressure behavior

1   Introduction

Computers have been used to solve fluid flow problems for many years.   Numerous programs have been written to solve either specific problems, or specific classes of problems.   From the mid-1970's, the complex mathematics required to generalize the algorithms began to be understood, and general purpose CFD solvers were developed.   These began to appear in the early 1980's and required what were then very powerful computers, as well as an in-depth knowledge of fluid dynamics, and large amounts of time to set up simulations. Consequently, CFD was a tool used almost exclusively in research.

As a result of these factors, Computational Fluid Dynamics is now an established industrial design tool, helping to reduce design time scales and improve processes throughout the engineering world.   CFD provides a cost-effective and accurate alternative to scale model testing, with variations on the simulation being performed quickly, offering obvious advantages.

ANSYS CFX is an advanced computational fluid dynamics (CFD) analysis tool that combines CAD input, automatic meshing, fast and advanced algorithms.   CFD is a computer-based tool for simulating the behaviour of systems involving fluid flow, heat transfer, and other related physical processes.   It works by solving the equations of fluid flow (In a special form) over a region of interest, with specified (known) conditions on the boundary of that region.

Numerical modeling of ventilation in living quarters, office space and utility rooms has been a subject of many scientific papers over the past few years (Abanto et al.,

2004; Evola and Popov, 2006; Lin et al., 2007; Stamou and Katsiris, 2006). Doing this kind of calculations allows an in-depth analysis of the ventilation issues already on the project stage, which significantly lowers the cost.

In this study, ANSYS-CFX workbench V12 was used to simulate the air action inside the negative pressure chamber. The tested seed plate of 1.8 mm hole diameter along with extra two plates with 2.2 mm and 2.5 mm seed holes were involved in the simulation. Negative pressure inlets with different shape and angles were also simulated in order to optimize the structure of the design. The setup was carried out with five levels of negative pressure used in laboratory testing including 2.5 kPa, 3.0 kPa, 3.5 kPa, 4.0 kPa and 4.5 kPa.

2   Literature reviews:

Xu Li et al., compared the results of dynamic analysis with simulation on sucking process of a pneumatic precision metering device for rapeseed using ANSYS-CFX, they proved that the outlet vacuum calculation model was completely correct.

Zhao et al. (2010) investigated the performance of a vacuum-cylinder seeder for the precision sowing of rapeseeds, they calculated the forces acting on the seeds in free flight using the computational fluid dynamics (CFD) software Fluent and numerically determined the seed motion, seeds falling trajectories of different working parameters using the differential equation, results of numerically computation and test-rig indicate good agreement. Deng et al. (2010) obtained some optimal results on the diameter of the nozzle, the nozzle number of the disc, the radius of orifice and the peripheral speed of the seed disc by analysis of the sucking-seed process of the nozzle of a pneumatic rapeseed-metering device and introducing an approximate model on the pressure difference of the nozzle. The theoretical results were verified by some experimental results. These studies were mostly carried out through combining empirical methods with experimental methods by many researchers. Examples of the application of theoretical model that defines the

relationship between the vacuity and design and operational parameters of the pneumatic precision metering device in the literature are limited.

Recent advances in computing power, together with powerful graphics and interactive 3D manipulation of models, have made the process of creating a CFD model and analyzing results much less labor intensive, reducing time and, hence, cost. Advanced solvers contain algorithms that enable robust solutions of the flow field in a reasonable time.

Hirt and Nichols (1981) developed a free surface capturing approach for finite volume CFD, where the amount of each fluid in a control volume is calculated in the solution process. Although this approach is computationally expensive it is robust and permits the simulation of highly non-linear free surface shapes, including fluid fragmentation and wave breaking. Most commercial CFD codes, including CFX, use this approach to include a free surface flow modeling capability.

3   Design background:

3.1   Determination of seed hole diameter

The seed hole of the metering disk was determined based on the $\leq 50\%$ size of geometric mean diameter of the wheat kernels according to R.C. Singh et al. (2005). The geometric mean diameter of the kernels was given by the following Equation 1:

$$ds = (lwt)^{\frac{1}{3}} \quad (1)$$

Where: ds is geometric mean diameter in mm; l, w and t are the mean length, width and thickness in mm, respectively.

3.2   Physical characteristics of wheat kernels:

The length, width and thickness were measured from 100 samples of randomly selected wheat kernels, as given in Table 1.

Table 1   Physical characteristics of wheat kernels

Physical properties	min	max	mean
Length l, mm	5.86	7.38	6.57
Width w, mm	3.10	3.88	3.63
Thickness t, mm	2.84	3.74	3.23
Geometric mean diameter m	3.81	4.51	4.19

3.3 Determination of QFI, MULI, MISI and KPM:

As stated by Singh et al. (2005), the evaluation of precision seeding (Table 2) and performance indices for laboratory experiment were calculated according to the following Equation 2 and Equation 3:

Table 2 evaluation of precision seeding according to the QFI percentage

Quality of Feed Index, %	Evaluation
> 98.6	Very good
> 90.4 – ≤ 98.6	Good
≥ 82.3 – ≤90.4	Moderate
< 82.3	Insufficient

Miss index:

The miss index I_{miss} is the percentage of spacing greater than 1.5 times the set planting distance S in mm.

$$I_{miss} = \frac{n_1}{N} \quad (2)$$

Where: n_1 is number of spacing > 1.5 S; and N is total number of measured spacing.

Multiple indexes:

The multiple index I_{mult} is the percentage of spacing that are less than or equal to half of the set plant distance S in mm.

$$I_{mult} = \frac{n_2}{N} \quad (3)$$

Where: n_2 is number of spacing ≤ 0.5 S.

Quality of feed index:

The quality of feed index I_q is the percentage of spacing that are more than half but not more than 1.5 times the set planting distance S in mm. The quality of feed index is an alternate way of presenting the performance of misses and multiples (see Equation 4).

$$I_{fq} = 100 - (I_{miss} + I_{mult}) \quad (4)$$

Theoretical real seed spacing RSS:

The theoretical real seed spacing (Table: 3 and Table 4) was obtained from the following Equation 5:

Table 3 Duncan's multiple range test for variables under influence of negative pressure

NP	QFI	MULI	MISI	KPM
2.5	83.59 [a]	3.64 [a]	12.77 [a]	32 [a]
3.0	83.84 [a]	6.26 [a]	10.56 [b]	35 [a]
3.5	85.41 [b]	9.12 [a]	5.46 [c]	37 [b]
4.0	87.42 [b]	9.99 [b]	2.60 [d]	42 [c]
4.5	87.51 [b]	10.04 [c]	2.38 [d]	43 [d]

Note: Means with the same letter are not significantly different

Table 4 The quality of feed index (QFI), multiple index (MULI), miss index, average seed spacing and number of plants/m according to the field data

Ave. FWS, km/h			2.10		
Ave. RS, rpm			18.00		
RSS, mm			64.00		
Rep.	Ave. seed spacing, mm	No. of plants/m	QFI%	MULI%	MISI%
R1	61.50	17	69.50	18.00	12.50
R2	61.30	16	66.60	13.30	20.00
R3	90.50	15	71.40	0.00	28.50
R4	95.50	16	73.30	13.3	13.30
R5	52.10	11	70.00	0.00	30.00
R6	56.70	19	85.70	14.20	0.00
R7	58.00	20	73.60	15.70	10.50
R8	39.30	21	80.00	10.00	10.00
R9	50.30	23	68.18	27.27	4.54
R10	62.60	29	64.28	25.00	10.70
mean	62.50	18.00	72.25	13.67	14.00

$$RSS = \frac{FWS}{3.6} \times \frac{60}{RS} \times \frac{1}{N} \times 1000 \quad (5)$$

Where: RSS is real seed spacing in mm, FWS is forward speed in km/h, RS is rotating speed in rpm, and N is number of holes of the seed plate.

4   Simulation process

The results of the simulation have been obtained through several steps:

The geometry (Figure 1) of the gas area inside the pressure chamber was built on ZX Plane using fluid flow design Modeler.   According to the real dimensions total width of the pressure chamber was made 25 mm, the pressure inlet having a diameter of 20mm was drawn at 12.5 mm whereas the seed holes were positioned at 15.5 mm.
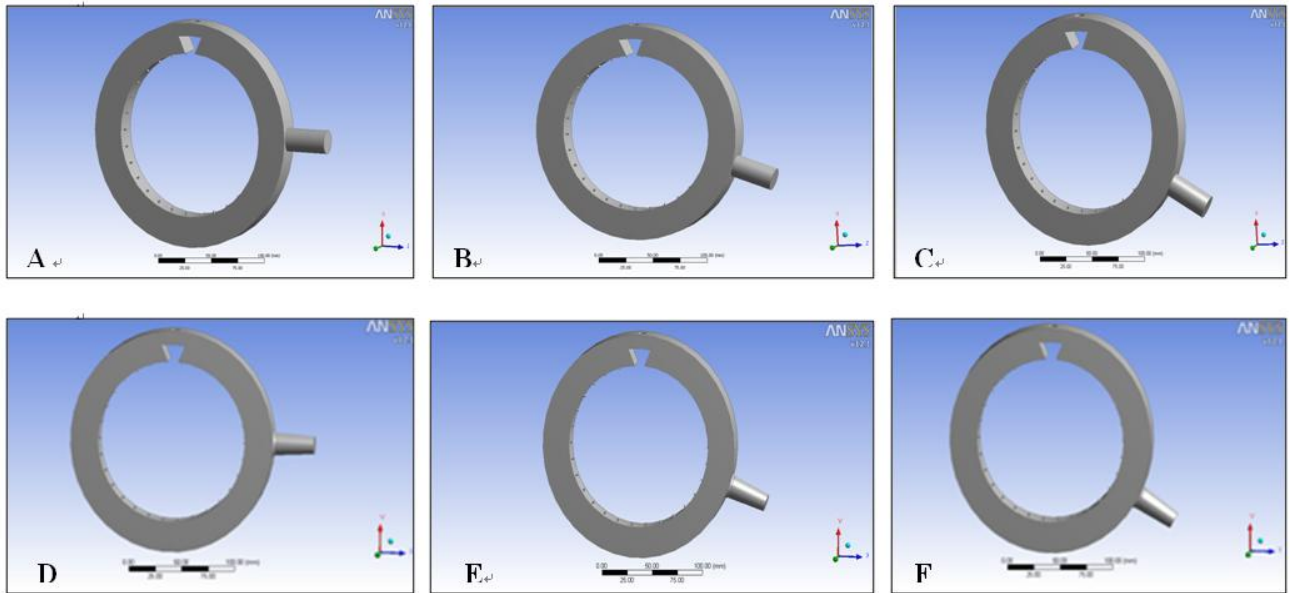
Figure 1   Geometry building using ANSYS-CFX designModeler
A: cylindrical pressure inlet, B: cylindrical pressure inlet with 20 °, C: cylindrical pressure inlet with 30 °,
D: revolved pressure inlet, E: revolved pressure inlet with 20 °, F: revolved pressure inlet with 30 °

For accurate results fine meshing was selected, the inlet (seed holes) and outlet (negative pressure port) were defined as regions with maximum spacing of 1.7 mm, a layer was also added to the part of PVC cut-off device with maximum thickness of 1.5 mm, then the surface and volume meshing were generated (Figure 2).
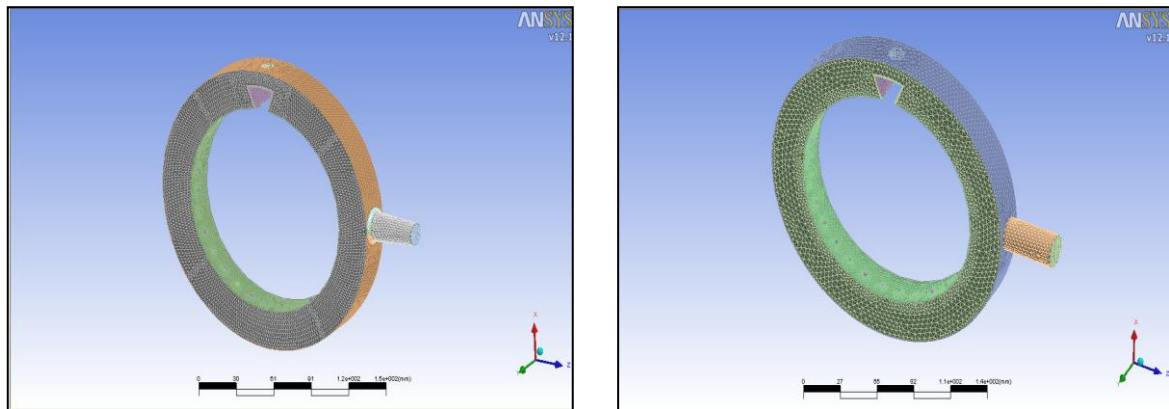

Figure 2   Meshing cells and layer around PVC cut-off device

On the CFX-Pre (setup stage), the inlet and outlet were defined as boundaries choosing opening as a boundary type, the relative pressure was set at 0 Pa for the inlet (seed holes) whereas, for the outlet one value out of five levels (-2500, -3000, -3500, -40000 and -4500) was selected for every individual running.

In this stage the solver control was to be set, physical timescale at two second was chosen for timescale control with minimum and maximum interactions ranging from one to 100 respectively (Figure 3).
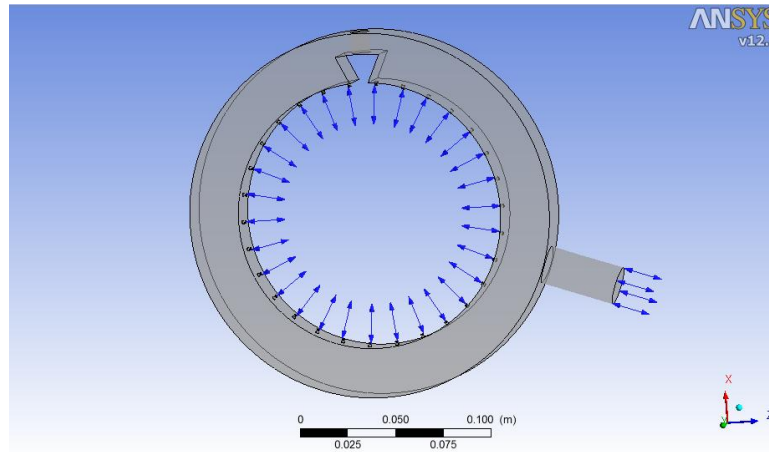
Figure 3   Defining the boundaries

After doing the required setting the CFX solver manager (Figure 4) has to be run and the results were then obtained as a contour map in the CFX-CFD-Post stage.
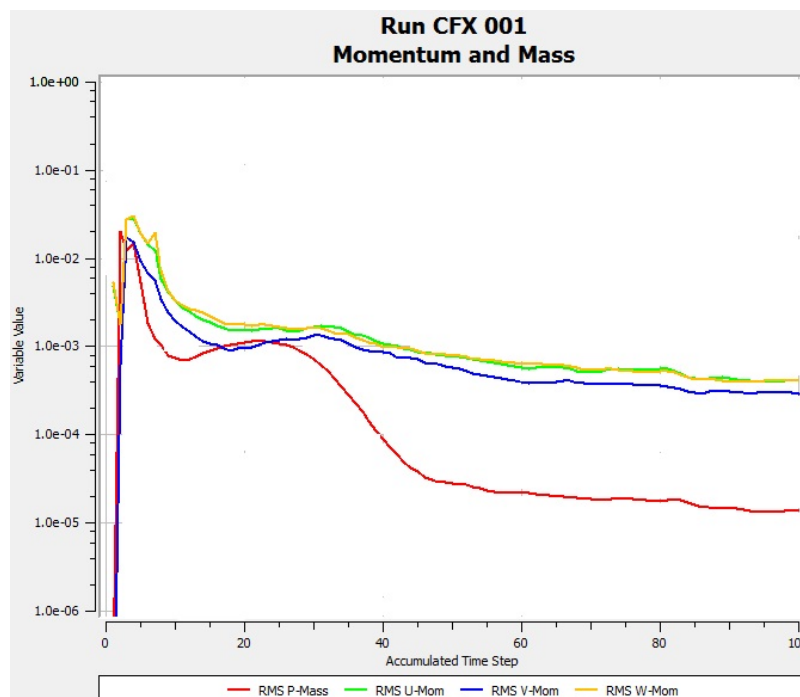
Figure 4   Stability on the CFX solver manager graph

5   Results of simulating cylindrical and revolved pressure inlet using a seed plate with 1.8 mm under 2.5 kPa negative pressure

Looking attentively to Figure 5, it can be observed that the pressure was stable with both cylindrical pressure inlet and angled cylindrical pressure inlet of 20° (indicated by green colour), in the later the uniform colours appear to cover the both sides of the pressure chamber, however, the former looked more suitable as the stability of vacuum pressure cover the targeted seed holding, transmitting and releasing area, whereas in the angled cylindrical inlet of 30° the pressure is a little bit higher in the lower part of the rightward side according to the contour map.
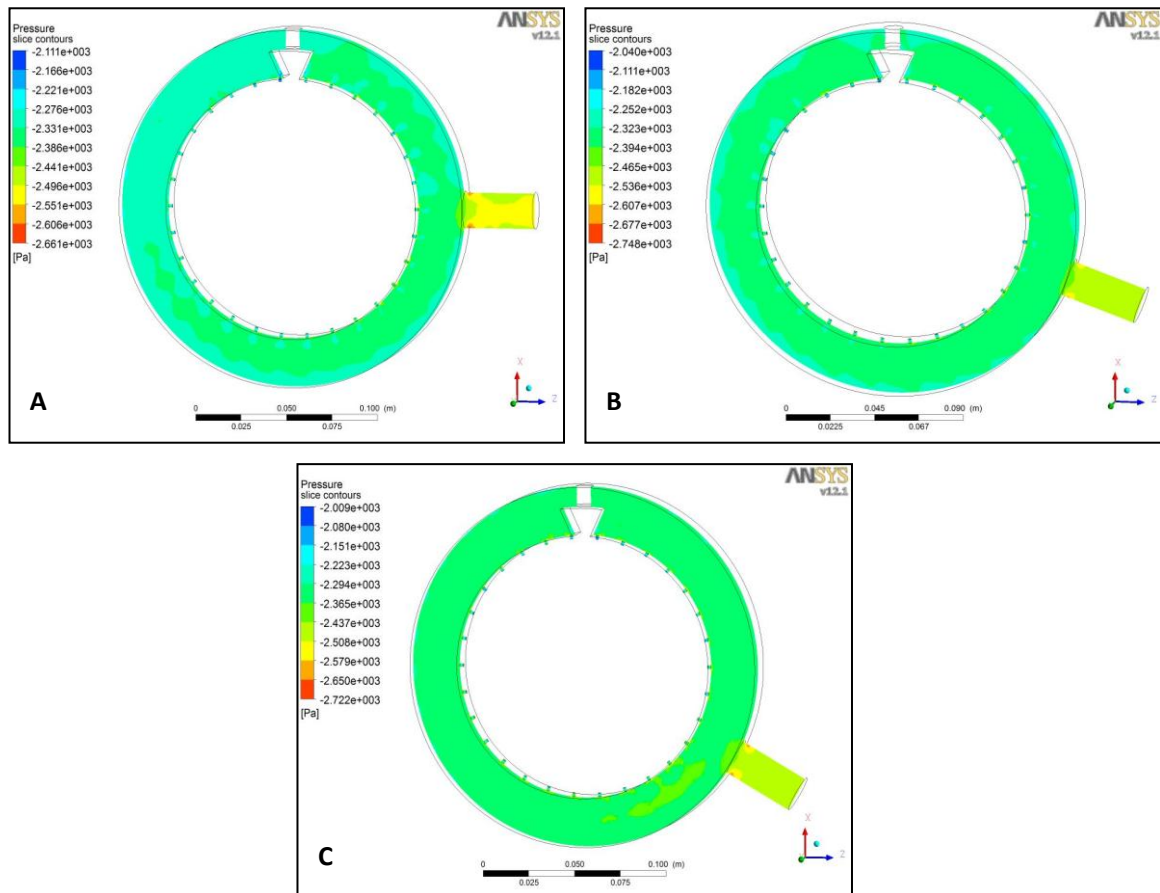
Figure 5   Simulation of different positions of cylindrical pressure inlet with 1.8 mm seed holes and 2.5 kPa negative pressure

A: cylindrical pressure inlet, B: cylindrical pressure inlet with 20°, C: cylindrical pressure inlet with 30°

For the revolved inlet (Figure 6), the pressure is observed to be more stable in revolved inlet (Figure 6-A) rather than the other two inlets within which turbulence is occurred (Figure 6-B and 6-C) revealed in yellow colour.
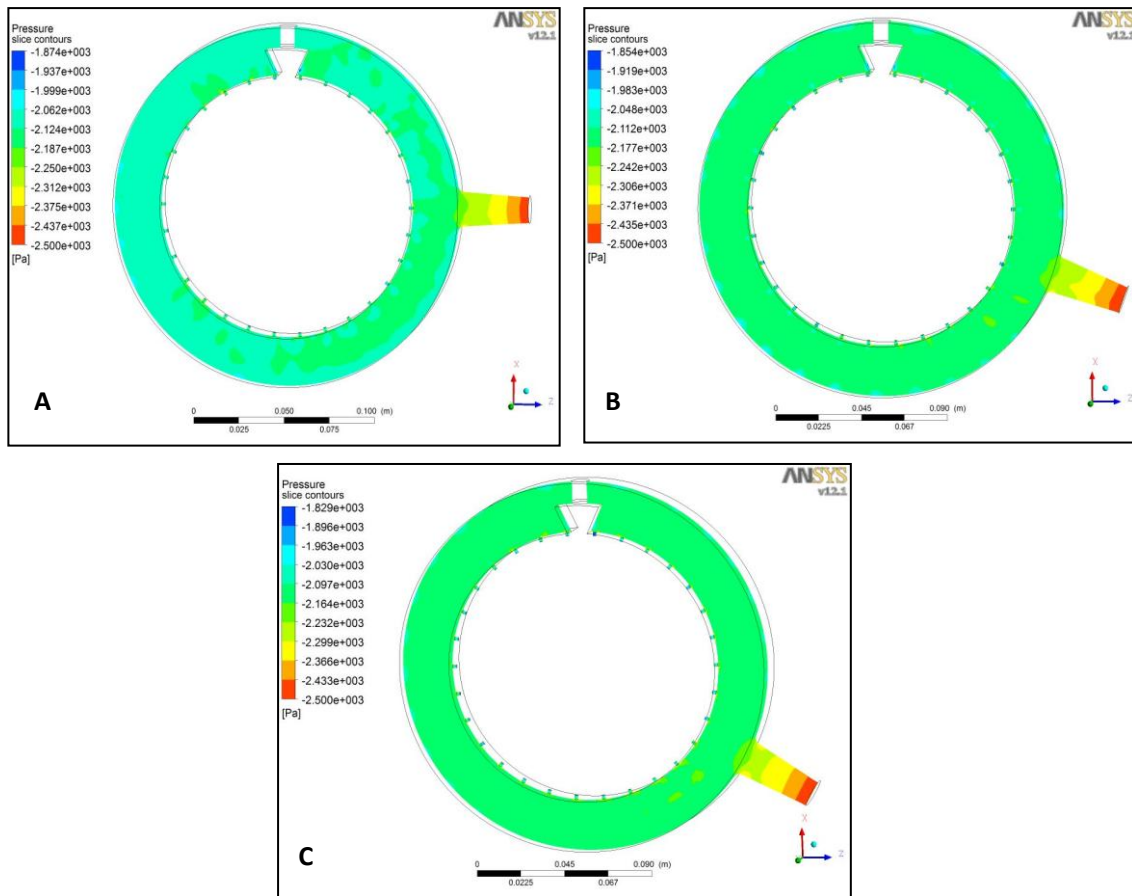
Figure 6   Simulation of different positions of revolved pressure inlet with 1.8 mm seed holes and 2.5 kPa negative pressure

A: revolved pressure inlet, B: revolved pressure inlet with 20 °, C: revolved pressure inlet with 30 °

Due to the curved (blended) inside edge of the inlet pressure, it can be observed that the high pressure exists only in the outside edge

6   Simulation of different pressure inlets and different seed holes with 2.5 kPa negative pressure

In this section different pressure inlets with different seed hole diameters were simulated based on 2.5 kPa negative pressure.

6.1   Revolved pressure inlet

The simulation results of all types of revolved pressure inlet including the angled of 20 and 30 degrees are revealed in Figure 7, Figure 8 and Figure 9.
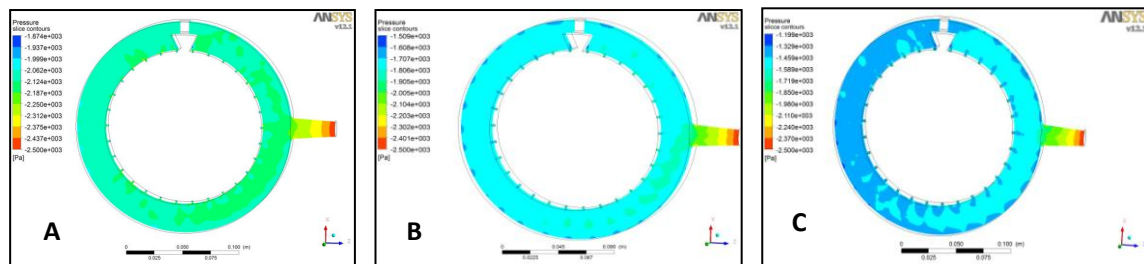

Figure 7   Revolved pressure inlet

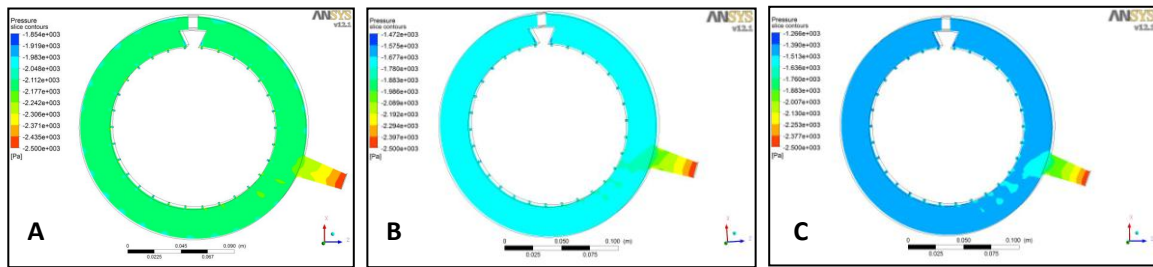A: 1.8mm, B: 2.2 mm, C: 2.5 mm

Figure 8   Revolved pressure inlet with 20 °
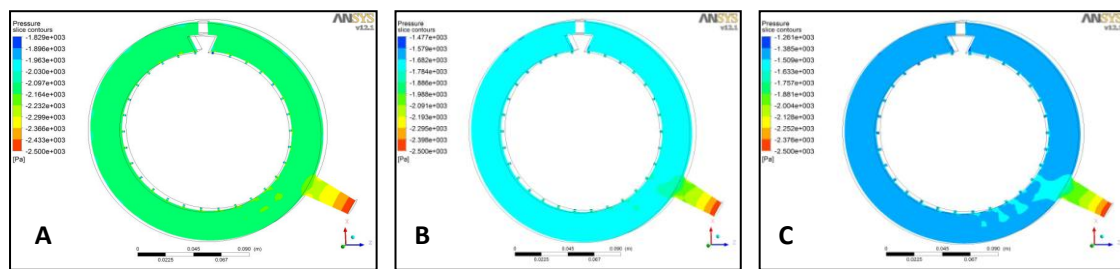
A: 1.8mm, B: 2.2 mm, C: 2.5 mm

Figure 9   Revolved pressure inlet with 30 °

A: 1.8mm, B: 2.2 mm, C: 2.5 mm

Among the three positions of this type the best stability of the negative pressure was given by the seed plate of 1.8 mm seed hole.

6.2   Cylindrical pressure inlet

Figure 10 demonstrates the pressure behaviour with 1.8 mm, 2.2 mm and 2.5 mm seed holes when the cylindrical inlet is used.   The simulation result exposed a stable pressure with 1.8 mm seed hole, in Figure 10-A, over the area of seed metering (rightward) the pressure was almost 2.3 kPa.   With 2.2 mm seed hole a relatively stable pressure is provided, while turbulence is obviously observed with 2.5 mm seed hole
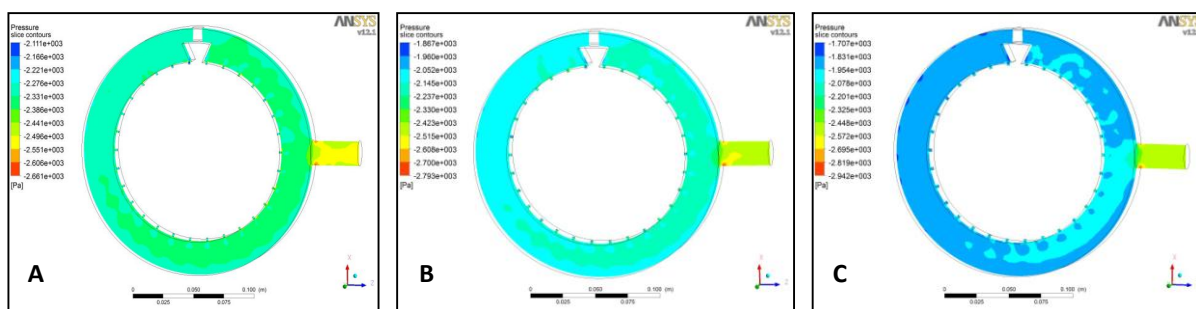

Figure 10   Cylindrical pressure inlet

A: 1.8mm, B: 2.2 mm, C: 2.5 mm

6.3   Cylindrical pressure inlet with 20 and 30 degrees

The behaviour of the negative pressure using both angled inlet is exposed in Figure 11 and Figure 12.

Similar to that of the cylindrical one, the pressure stability is apparently shown in seed plate of 1.8 mm seed hole likewise the seed plate of 2.2 mm seed hole within which the pressure is relatively stable, whereas in the seed plate of 2.5 mm seed hole more turbulence is observed.
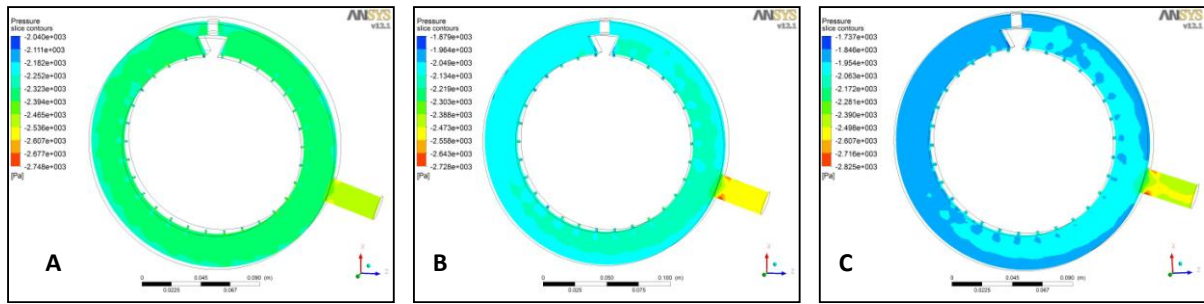
Figure 11   Cylindrical pressure inlet with 20 °
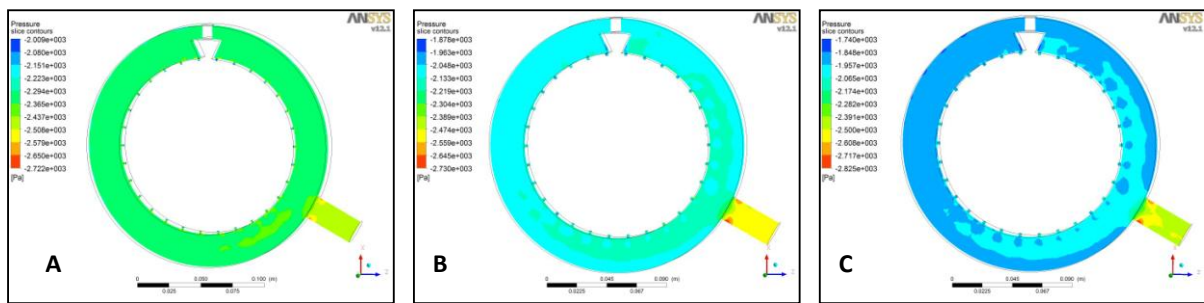
A: 1.8mm, B: 2.2 mm, C: 2.5 mm

Fig.12: Cylindrical pressure inlet with 30 °

A: 1.8mm, B: 2.2 mm, C: 2.5 mm

7   Simulation of cylindrical pressure inlet and 1.8 mm seed hole under different levels of negative pressure

Based on the ANSYS-CFX results and geometric mean diameter, the cylindrical pressure inlet with seed plate of 1.8 mm hole diameter were selected as the best among other tested structures regarding the stability of the negative pressure on the targeted area up on which the process of seed metering is accomplish.   Accordingly, they had been simulated over the range of seed holes (15.5 mm).

The simulation results of the cylindrical pressure inlet and 1.8 mm seed plate with different levels of negative pressure (2.5 kPa, 3.0 kPa, 3.5 kPa, 4.0 kPa and 4.5 kPa) are highlighted in Figure 13 and 14.
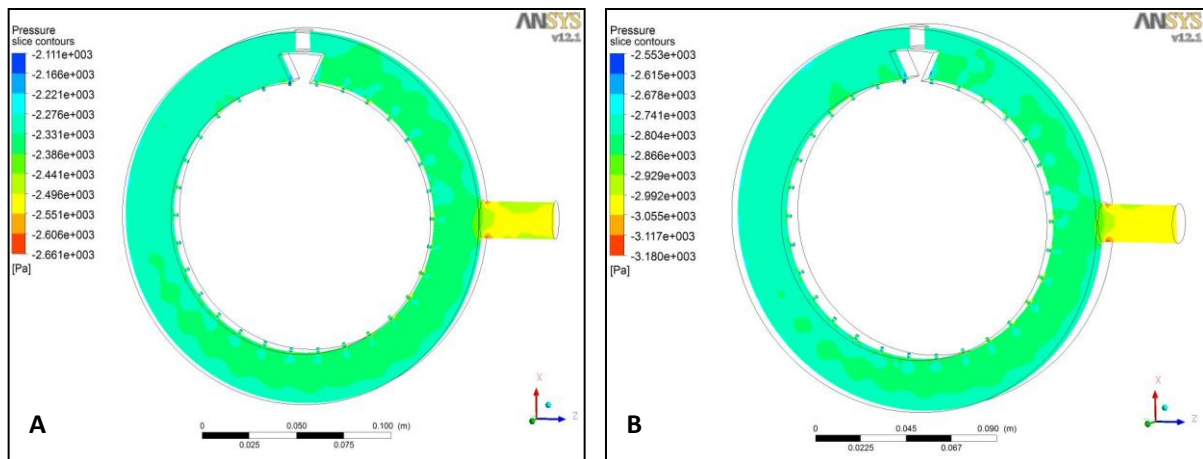

Figure 13   Contour map showing the pressure chamber of the precision metering device for wheat under different levels of negative pressure
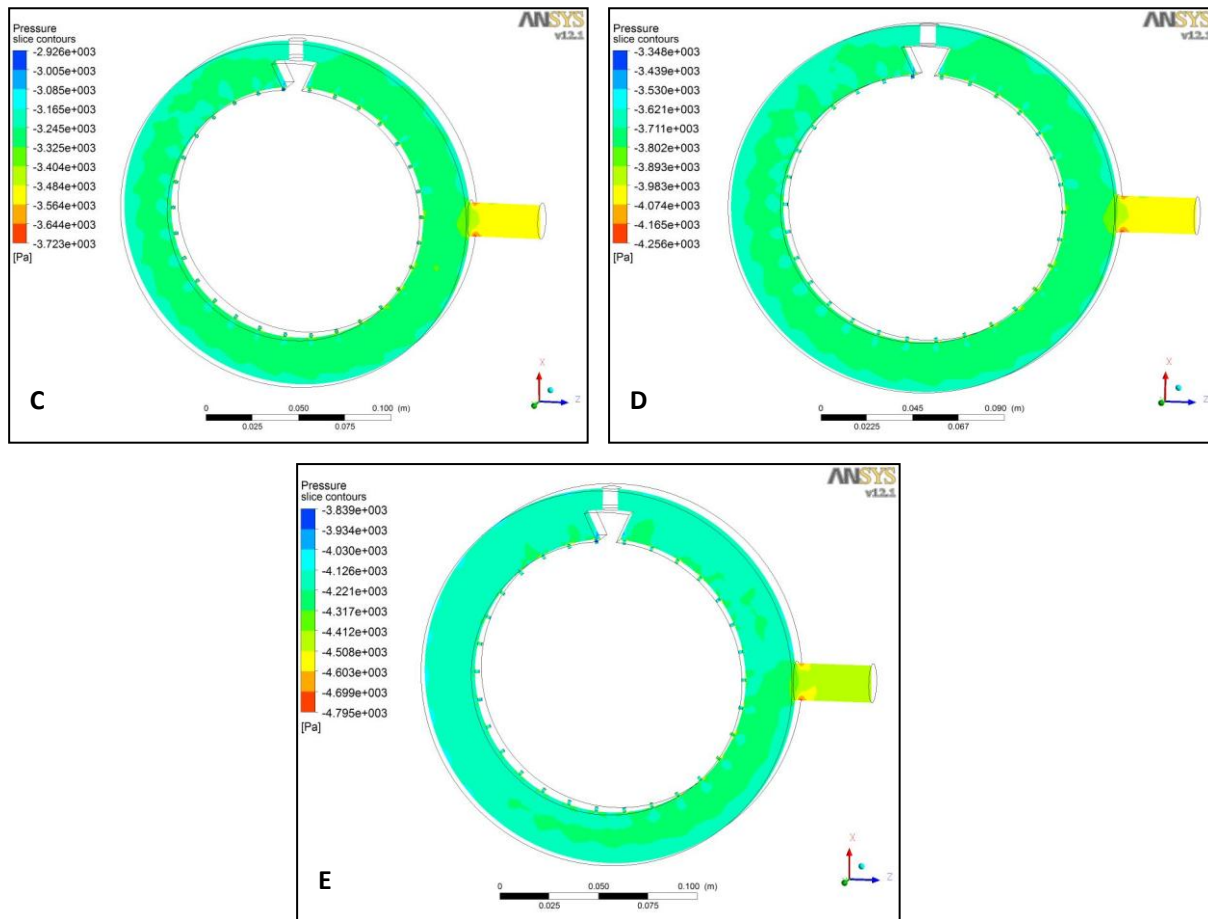A: 2.5 kPa, B: 3.0 kPa

Figure 14   Contour map showing the pressure chamber of the precision metering device for wheat under
different levels of negative pressure
C: 3.5 kPa, D: 4.0 kPa, E: 4.5 kPa

The contour colours exposed a high pressure in inlet port especially at the end; this may be due to the high friction caused by the sharp insider edge of the inlet port in this position. The heat generated may influence the efficiency of the air by decreasing the viscosity.

The most important part on this device is the rightward half close to the pressure inlet because this part represent the area within which the kernels picked up and transport towards ejecting mechanism, thus, in this area it can be observed that the pressure is more stable (given in homogenous green colours).

Under all pressure levels involved in the test, the negative pressure was observed to be stable, particularly through seed holes, a little turbulence can be shown in case of 4.5 kPa negative pressure, which may attributed to the high pressure in the system.

8   design and manufacturing of the pneumatic precision metering device for wheat based on ANSYS-CFX results

As shown in Figure 15 and Figure 16, the device was firstly sketched as 3D and 2D using pro/Engineer wildfire v4 and CAXA software respectively, and then a prototype had been manufactured (Figure 17 and Figure 18). Hence, a laboratory experiments were conducted.
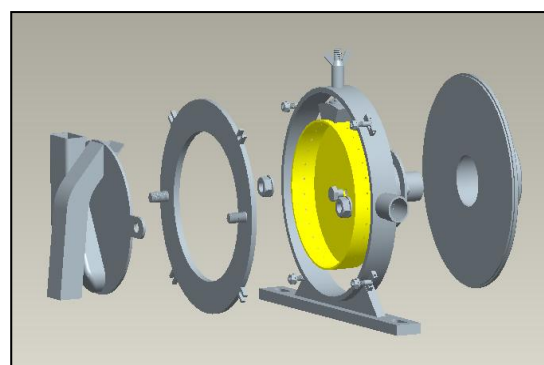

Figure 15   The new shield with hooked seed tube
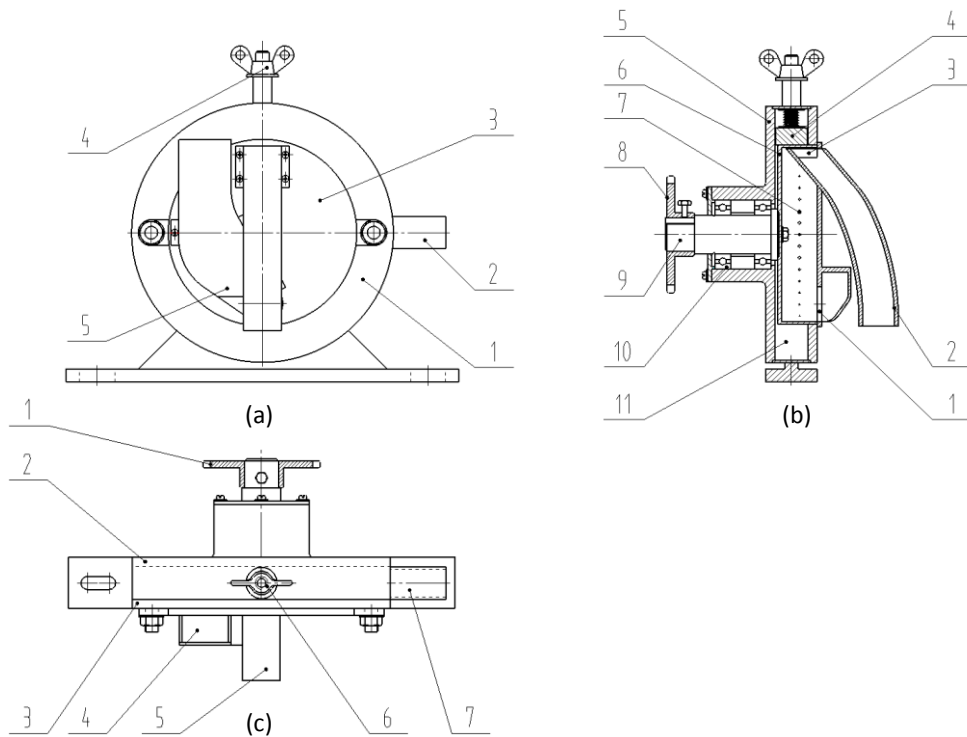sketched in Pro/ENGINEER

Fig.16: Schematic diagram of the pneumatic metering device with hooked seed tube

: (a): 1-removable steel ring 2-negative pressure inlet 3-removable shield
4-adjustable round wing nut 5-seed box, (b): 1-seed inlet 2-seed tube 3-seed outlet 4-spring loaded PVC air
cut-off device 5-main shield 6-seed plate 7-seed hole 8-gear 9-driving shaft   10-bearings 11-chamber of
negative pressure
(c): 1-gear, 2-main shield, 3- removable steel ring, 4-removable shield, 5-seed box, 6-seedtube, 7- adjustable
round wing nut, 8-negative pressure inlet
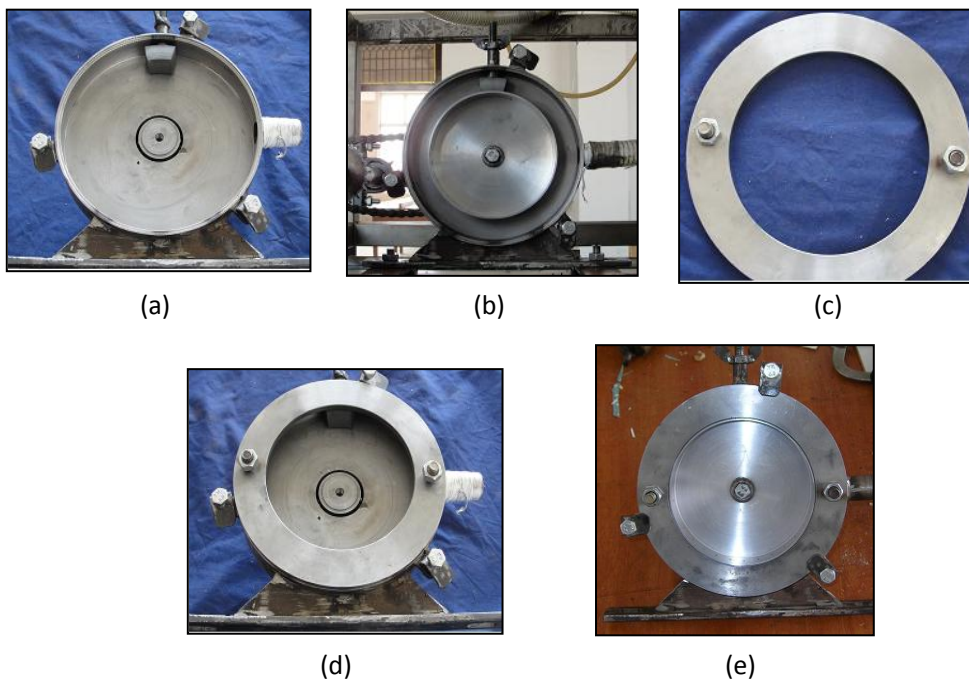

Figure 17   The main parts of the pneumatic precision metering device for wheat

(a): the main shield, (b): the main shield and seed plate, (c): the steel ring, (d): the main shield and ring, (e):
the main shield, seed plate and ring

Fig.18: The wheat seeder under laboratory testing using test stand with camera system

9   Results of the laboratory experiments for the pneumatic precision metering device for wheat:

Based on ANSYS-CFX results a prototype had been manufactured and tested under laboratory conditions, the results of these experiments are demonstrated in Table 3.

10   The results of field experiment

From Table 3, the QFI looked to be high enough for precision seeding even under the lowest negative pressure ranging from 83.59% minimum and 87.51% maximum for 2.5 kPa and 4.5 kPa negative pressures respectively (referred to Table 2).

Taking into account the unstable forward speed and negative pressure, the field experiment (Table 4) also revealed good results regarding the high values of QFI. From ANSYS-CFX results the pressure especially in the seed holes increases due to the increasing pressure in the whole system. From Table 3 and Table 4, the QFI increases while the MULI and MISI decreases when the negative pressure increases which indicates that the virtual structure derived from ANSYS-CFX results could give the same results in reality as shown in Table 3.

Conclusions

- Simulation with ANSYS-CFX and other similar softwares could accurately predict the behavior of negative pressure inside a pneumatic seeder and accordingly could decrease the cost of manufacturing.

- Using a seed hole less than or equal to 50% of the geometric mean diameter appear to be the best among other tested seed holes according to simulation and laboratory results which is in conformity with to R.C. Singh et al. (2005) findings.

- Both simulation and laboratory results were in agreement regarding to the increasing of QFI and decreasing of MULI and MISI when the negative pressure increases.

- Cylindrical pressure inlet stabilized the negative pressure in different levels as demonstrated in ANSYS-CFX contour maps as well as giving acceptable percentages of QFI, MULI and MISI as resulted from laboratory tests based on precision seeding criteria.

- Designing a cylindrical inlet with blended edge may give better results as well as proved in Figure 6.

- Irrespective of the relatively stable pressure in the gas chamber with revolved shape (Figure 6-A), however, a high pressure is emerged in the front part of the inlet which may overheat the gas and influence the pressure stability.

Recommendations:

- As revealed from simulation results (Figure 5-B), the cylindrical inlet with 20° had also produced a stable pressure, therefore, a further study including a hardware prototype might be needed to compare the results with similar parameters.

References

Abanto, J., D. Barrero, M. Reggio, and B. Ozell. 2004. Airflow modeling in a computer room, Building and Environment 39, 1393-1402 ANSYS-CFX Release 11.0: Theory, 2006.

Deng, X. Y., X. Li, C. X. Shu, H. D. Hang, and Q. X. Liao. 2010. Mathematical model and optimization of structure and operating parameters of pneumatic precision metering device for rapeseed. *International Journal of Food, Agriculture and Environment* 8(1): 318-322.

Hirt, C. W., and B. D. Nichols. 1981. Volume of fluid (VOF) method for the dynamics of free boundaries. *Journal of Computational Physics*, 39: 201–225.

Singh, R. C., G. Singh, and D. C. Saraswat. 2005. Optimization of design an operational parameters of a pneumatic seed metering device for planting cottonseeds. *Biosystems Engineering,* 92(4): 429-438.

Li, X, Q. X. Liao, J. J.Yu, C. X. Shu, and Y. T. Liao. 2012. Dynamic analysis and simulation on sucking process of pneumatic precision metering device for rapeseed. *Journal of Food, Agriculture & Environment,* 10 (1): 450-454.

Zhao, Z., Y. M. Li, J. Chen, and L. Z. Xu. 2010. Numerical analysis and laboratory testing of seed spacing uniformity performance for vacuum- cylinder precision seeder. *Biosystems Engineering,* 106(4): 344-351.